Comparative Genomic Analysis of *Acinetobacter oleivorans* DR1 To Determine Strain-Specific Genomic Regions and Gentisate Biodegradation[∇][†]

Jaejoon Jung,[1] Eugene L. Madsen,[2] Che Ok Jeon,[3] and Woojun Park[1]*

Department of Environmental Science and Ecological Engineering, Korea University, Anam-Dong 5 Ga, Seungbuk-Ku, Seoul, Republic of Korea 136-713[1]; Department of Microbiology, Cornell University, Ithaca, New York 14853-8101[2]; and Department of Life Science, Chung-Ang University, Seoul, Republic of Korea 156-756[3]

The comparative genomics of *Acinetobacter oleivorans* DR1 assayed with *A. baylyi* ADP1, *A. calcoaceticus* PHEA-2, and *A. baumannii* ATCC 17978 revealed that the incorporation of phage-related genomic regions and the absence of transposable elements have contributed to the large size (4.15 Mb) of the DR1 genome. A horizontally transferred genomic region and a higher proportion of transcriptional regulator- and signal peptide-coding genes were identified as characteristics of the DR1 genome. Incomplete glucose metabolism, metabolic pathways of aromatic compounds, biofilm formation, antibiotics and metal resistance, and natural competence genes were conserved in four compared genomes. Interestingly, only strain DR1 possesses gentisate 1,2-dioxygenase (*nagI*) and grows on gentisate, whereas other species cannot. Expression of the *nagI* gene was upregulated during gentisate utilization, and four downstream open reading frames (ORFs) were cotranscribed, supporting the notion that gentisate metabolism is a unique characteristic of strain DR1. The genomic analysis of strain DR1 provides additional insights into the function, ecology, and evolution of *Acinetobacter* species.

Acinetobacter species have been isolated from a variety of habitats, including seawater, activated sludge, human clinical specimens, cotton, and soils, suggesting the profound adaptability of the genus to various environments and its ubiquity. Genomic research on *Acinetobacter* has largely focused on *A. baumannii* strains due to the clinical importance of multidrug-resistant (MDR) strains (37). Currently, eight complete genomes of *A. baumannii* strains are available, whereas only three environmental strains—*A. baylyi* ADP1, *A. calcoaceticus* PHEA-2, and *A. oleivorans* DR1—had been sequenced at the time the current paper was prepared (4, 15, 38). The NCBI Genome Project has reported that 83 genomes of *Acinetobacter* (77 clinical strains) are currently being sequenced. Comparative genomic studies have highlighted a variety of relevant genetic contrasts between soil-isolated *A. baylyi* ADP1 and MDR *A. baumannii* strains; many differences in metabolic capacities, quorum-sensing systems, nutrient acquisition, and mobile genetic elements were identified (1, 10, 35). Environmental isolates of *Acinetobacter* species are expected to harbor biotechnologically and environmentally important genes encoding, e.g., extracellular lipase and biosurfactants and novel genes for contaminant degradation, owing to their broad range of metabolic capacities (6, 17, 22). However, genomic contrasts among environmental *Acinetobacter* species and their ecological implications have yet to be thoroughly elucidated.

The novel diesel-degrading strain *Acinetobacter oleivorans* DR1 was isolated from rice paddy soil (18). The genetics and physiology of strain DR1 (with respect to activities such as biodegradation of diesel fuel, biofilm formation, natural transformation, quorum sensing, and oxidative stress) have only begun to be investigated (16, 19, 20, 21, 30). The availability of the complete genome of strain DR1 (16) provides the opportunity for a comparative study. Here, the genome of *A. oleivorans* DR1 was intensively compared to those of *A. baylyi* ADP1, *A. calcoaceticus* PHEA-2, and *A. baumannii* ATCC 17978. The metabolism of gentisate exhibited by strain DR1 (and absent in all the other *Acinetobacter* strains) is also described herein.

The genomes of *A. oleivorans* DR1 KCTC 23045[T], *A. baylyi* ADP1 (hereafter *A. baylyi*), *A. calcoaceticus* PHEA-2 (hereafter *A. calcoaceticus*), and *A. baumannii* ATCC 17978 (hereafter *A. baumannii*) were compared throughout this study. The NCBI genome, Integrated Microbial Genomes (IMG), and Kyoto Encyclopedia of Genes and Genomes (KEGG) pathway databases were the primary sources used for predictions and comparisons. *A. oleivorans* DR1 possesses a larger genome than any other *Acinetobacter* species sequenced to date (Table 1; see also Fig. S1 in the supplemental material). Among the four strains whose genomes were examined, *A. baumannii* was the only one found to harbor pseudogenes (note that data concerning pseudogenes, clustered, regularly interspaced, short palindromic repeats [CRISPRs], and horizontally transferred genes of *A. calcoaceticus* were not determined due to the absence of the *A. calcoaceticus* genome from the IMG database at the time of manuscript preparation). A1S_0206 and A1S_0210 encode nonfunctional ATPases and are disrupted via insertion. Transposases located in the proximity of these two pseudogenes may constitute evidence of the insertion

---

TABLE 1. Main features of the genome[a]

Characteristic	Value(s)			
	A. oleivorans DR1	*A. baylyi*	*A. calcoaceticus*	*A. baumannii*
Total size (bp)	4,152,543	3,598,621	3,862,530	4,001,457
No. of plasmids	None	None	None	2 (pAB1 [13,408 bp]; pAB2 [11,302 bp])
No. of DNA coding bases (bp) (% of total length)	3,646,889 (87.8)	3,195,476 (88.8)	3,374,434 (87.4)	2,898,244 (72.4)
G+C content (%)	38.7	40.4	38.8	Chromosome, 38.9; pAB1, 36.2; pAB2, 35.2
No. of protein-coding genes	3,874	3,325	3,095	3,370
rRNA (16S–tRNA^{Ile}–tRNA^{Ala}–23S–5S)	6 operons	7 operons	2 operons	5 operons
tRNA	71	76	69	70
Average gene length (bp)	934	955	938	Chromosome, 888; pAB1, 692; pAB2, 1211
No. (%) of protein-coding genes with function prediction	2,746 (69.3)	2,090 (60.9)	1,981 (64.0)	2,507 (72.4)
No. (%) of protein-coding genes with COG	2,932 (74.0)	2,090 (60.9)	2,483 (80.2)	2,716 (78.4)
No. of pseudogenes	None	None	Not available	2

[a] The information regarding the *A. baylyi*, *A. calcoaceticus*, and *A. baumannii* genomes is presented for comparison. The information pertaining to *A. oleivorans* DR1, *A. baylyi*, and *A. baumannii* is available on the IMG website (http://img.jgi.doe.gov). The information regarding *A. calcoaceticus* was either derived from the study of Zhan et al. (38) or calculated in this study.

event. Analysis of clusters of orthologous groups (COG) revealed that the genes involved in transcription comprised the dominant group encoding proteins in the DR1 genome, whereas those encoding amino acid transport- and metabolism-related proteins accounted for the largest portion in *A. baylyi*, *A. calcoaceticus*, and *A. baumannii* (see Fig. S2 in the supplemental material). Interestingly, strain DR1 harbors 1,283 signal peptide-encoding genes (32.4%), whereas 251 (7.3%) and 621 (18.1%) such genes were noted in *A. baumannii* and *A. baylyi*, respectively. Genes encoding peptides such as biofilm synthesis proteins (AOLE_06345 and AOLE_14665), efflux pumps (AOLE_00050, AOLE_00530, AOLE_02025, AOLE_09285, and AOLE_09410), proteases (AOLE_03750, AOLE_03780, and AOLE_04795), and a variety of transporters have been identified in the DR1 strain. Tightly associated catabolic gene clusters have been noted as a feature of *A. baylyi* (4). As demonstrated in Fig. 1, the protocatechuate branch of the β-ketoadipate pathway, quinate, 4-hydroxybenzoate, and ferulate genes are adjacently arranged in *A. baylyi*. The benzoate and catechol branches of the β-ketoadipate pathway are also adjacent to one another. In strain DR1, *A. calcoaceticus*, and *A. baumannii*, catabolic genes evidence a concentrated arrangement. However, their arrangement is not as tight as that observed in *A. baylyi*. Catabolic gene islands are regarded as beneficial for efficient metabolism (4).

A. oleivorans DR1 does not harbor glucokinase, 6-phosphofructokinase, pyruvate kinase, or the Glc, Lac, Man, and Fru family phosphotransferase system, with the exception of FruAB. Incomplete glucose metabolism in strain DR1 is consistent with the inability of DR1 to utilize glucose as a sole carbon source as well as with the results of previous comparative genomic studies of *A. baumannii* AYE and SDF and *A. baylyi* ADP1. In the pentose phosphate pathway, β-D-fructose 6-phosphate, rather than D-glucose or D-gluconate, is a precursor of D-ribose 5-phosphate, the starting material of nucleic acid metabolism. All components of the citric acid cycle were present. Isocitrate lyase (AOLE_14300) and malate synthase G (AOLE_10740), constituting the glyoxylate shunt, were pre-

viously identified (16). Among the biosynthetic pathways for 20 amino acids, the tyrosine pathway was incomplete because cyclohexadienyl dehydrogenase (which converts L-arogenate to tyrosine) was absent. Additionally, aspartate-ammonia lyase and asparagine synthase were not identified in the L-asparagine biosynthesis pathway. The biosynthesis pathways of all the other amino acids were present in strain DR1.
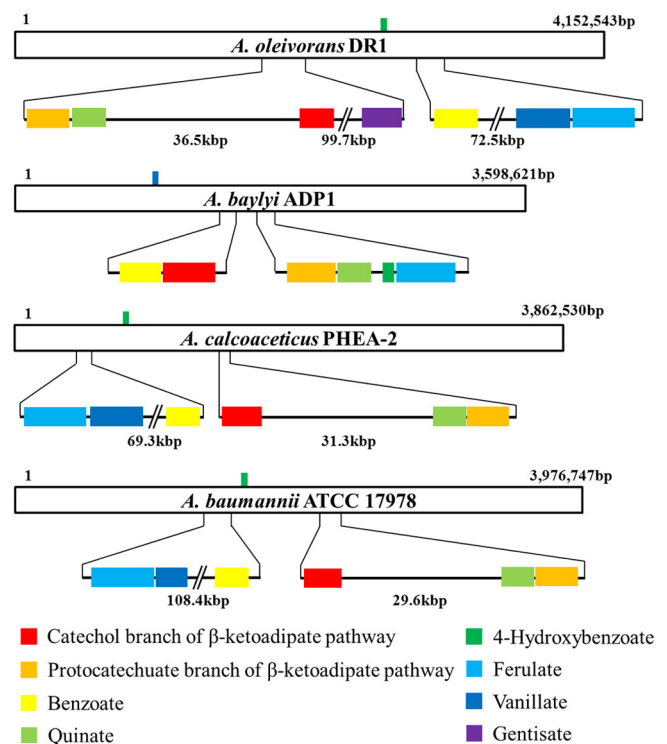

FIG. 1. Locations of catabolic gene clusters. The length of each white bar represents the relative length of each chromosome. Bars with colors indicate the locations of gene clusters on the chromosome. Distances between gene clusters are designated.
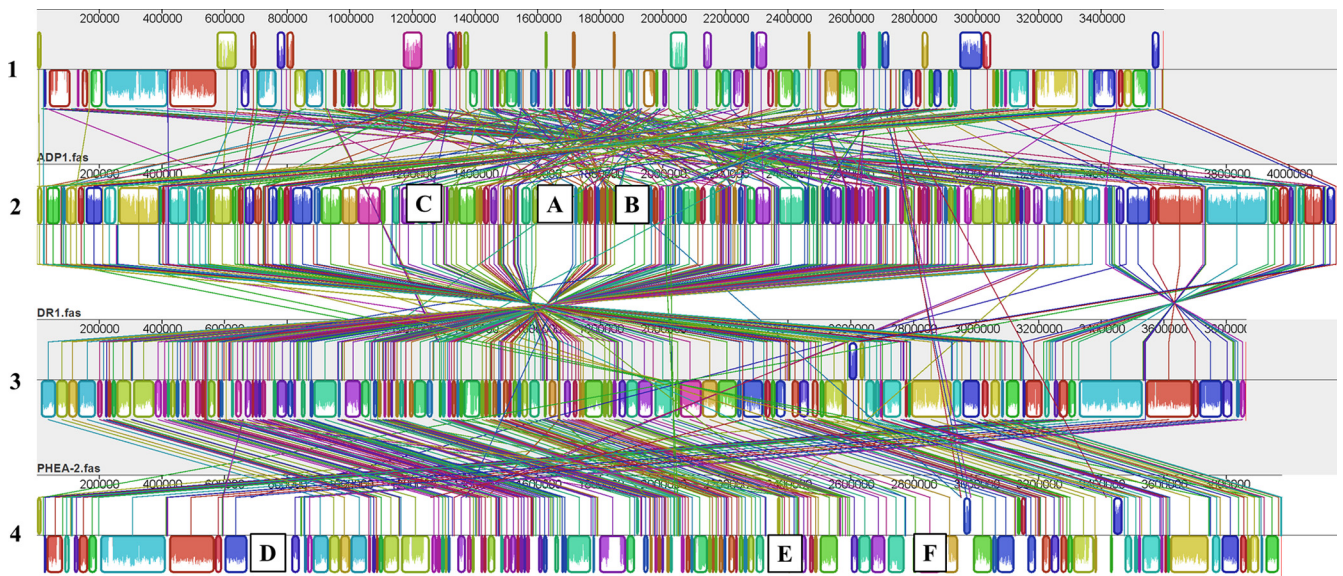
FIG. 2. Multiple genome alignment performed using Mauve software and the chromosomes of *A. oleivorans* DR1, *A. baylyi*, *A. calcoaceticus*, and *A. baumannii*. *A. oleivorans* DR1 is the reference for alignments and comparisons to the three other strains. Boxes with identical colors represent local colinear blocks (LCB), indicating homologous DNA regions shared by two or more chromosomes without sequence rearrangements. LCBs indicated below the horizontal black line represent reverse complements of the reference LCB. Six unmatched regions are designated with letters and represent strain-specific regions. 1, *A. baylyi*; 2, *A. oleivorans* DR1; 3, *A. calcoaceticus*; 4, *A. baumannii*.

The *soxR* transcriptional factor has been well characterized in *Escherichia coli* as an oxidative stress response regulator that thus activates *soxS* and subsequent regulons that function in the removal of superoxide, nitric oxide, and the stress induced by organic solvents and antibiotics. However, uncertainties regarding the established SoxR-SoxS paradigm have recently arisen due to evidence from *Pseudomonas aeruginosa* studies (8). To provide insight into the *soxR* system in strain DR1, we derived the consensus sequence of *soxR* boxes (5′-TTGACYT CAASTKAASTTKARSTTKS-3′) according to *in silico* analysis (9). Within the promoter region of AOLE_16635 (encoding a hypothetical protein) and upstream of AOLE_18445 (encoding a SoxR family transcriptional regulator), *soxR* boxes were identified in the strain DR1 genome. The BLAST matches to AOLE_16635 harbor the conserved domain YjgF and cluster with eight YjgF family translation inhibition inhibitors (NCBI protein cluster CLSK707763). Homologues of AOLE_18445 (SoxR family transcriptional regulator) have a conserved CueR domain that is found in the Cu(I)-responsive transcriptional regulator of the copper efflux system. The protein encoded by AOLE_14380 evidences 35% amino acid sequence similarity to the *E. coli* oxyR-encoded protein, another important transcriptional regulator involved in oxidative stress. The protein encoded by AOLE_14380 harbors the OxyR consensus sequence (LILLEEGHCLRDHVLSAC [18 amino acids]) (12). In the case of *A. baylyi*, *oxyR* was known to comprise an operon with the upstream rubredoxin gene. However, the OxyR binding site (ATAG-n7-CTAT-n7-ATAG-n7-CTAT) required for self-regulation was not detected in the promoter region of AOLE_14364, coding for rubredoxin. Many oxidative stress-related genes, such as catalase (AOLE_09800, AOLE_11770, AOLE_12755, and AOLE_17390) and superoxide dismutase (AOLE_01750 and AOLE_05305), have been identified. Glutaredoxin (AOLE_08120 and AOLE_16785) and thioredoxin

(AOLE_02585, AOLE_07635, AOLE_15340, and AOLE_16430) were shown to be clustered with *Acinetobacter* glutaredoxins and thioredoxins, respectively, whereas AOLE_19220 was also phylogenetically related to the thioredoxins of *A. baylyi* (ACIAD0045), *Moraxella*, and *Psychrobacter* species.

The genomes of strain DR1, *A. baylyi*, and *A. baumannii* were aligned using Mauve software (7). The majority of genes in the DR1 genome are arranged in the opposite direction from those of *A. calcoaceticus* and *A. baumannii*, whereas the genes in the ADP1 genome are arranged in a rather irregular pattern relative to the DR1 genome (Fig. 2). The alignment of the DR1 genome revealed that six large genomic regions did not have significant matches in other genomes; those are referred to here as DR1-specific genomic regions A, B, and C and *A. baumannii*-specific genomic regions D, E, and F (Fig. 2). Region A (approximately bp 1605202 to 1718447 [113 kb]) harbors 93 (75.6%) hypothetical proteins among 123 coding sequences (CDSs), with a variety of phage-related sequences corresponding to the phage integrase, prophage transcriptional regulator, phage DNA methylase, and Mu-like prophage proteins. The composition of this region is similar to that of the phage-related islands of *Staphylococcus aureus*, *Pseudomonas aeruginosa*, and *Mycobacterium tuberculosis* strains, and yet their order was not relevant. A large portion of the hypothetical proteins and a GC content similar to that of the host are also consistent with the features of previous identified phage islands (23, 24, 28, 32). The presence of phage sequences in the DR1 genome prompted us to analyze the phage region in the remainder of the genome. The phage sequences were retrieved according to predicted functions and a BLAST search of the DR1, *A. calcoaceticus*, *A. baylyi*, and *A. baumannii* genomes. Cutoff values for defining homologues were more than 30% amino acid identity, 70% coverage, and an E-value of less than 10^{-10}. Searched phage sequences and their homologues from

A. calcoaceticus, *A. baylyi*, and *A. baumannii* are listed in Table S1 in the supplemental material. Interestingly, aside from region A, the DR1 genome harbors another phage-related genomic region within bp 3195087 to 3224673. Our homologue search results indicated that this region is a homologue of one of the two phage regions found in *A. baylyi*. Regions D and E in *A. baumannii* (bp 697864 to 828937 and bp 2353055 to 2409240) are also phage islands encoding 90 hypothetical proteins among 171 CDSs, putative phage head morphogenesis, integrases, primases, transposases, and transposition helpers. Another DR1-specific genomic region (bp 2042729 to 2157853 [115 kb]; see region B in Fig. 2) harbored 31 (33.3%) genes encoding transport-related proteins among 93 coding sequences. COG categories suggest the presence of diverse transported substrates, including nitrate, sulfonate, bicarbonate, iron, biopolymer, peptides, and molybdate, along with multidrug transporter-related genes (AOLE_09700, AOLE_09705, and AOLE_09885). Two putative operons (AOLE_09680 to AOLE_09590 and AOLE_09625 to AOLE_09635) encoding TonB-ExbB-ExbD (involved in iron transport) were also located in this region (5). Interestingly, we identified genomic regions that had extremely low homology to counterpart genomes designated as regions C and F (bp 1106785 to 1137517 in DR1 [30 kb] and bp 2761467 to 2825021 in *A. baumannii* [63.6 kb]; Fig. 2). The features of region C (20 hypothetical proteins corresponding to a total of 35 CDSs) were not apparent. *A. baumannii* region F, however, appears to be dedicated to iron metabolism. A1S_2385 to A1S_2387 and A1S_2388 to A1S_2393 are described as iron metabolism genes. A1S_2387 harbors the ABC transporter involved in the iron-siderophore domain.

An insertion sequence (IS) may be the source of gene rearrangement and genome plasticity prompting genome evolution (2). Using the IS Finder tool, no matches were identified as insertion sequences in strain DR1. Regarding transposases, only two fragments (AOLE_05115 and AOLE_132325) were identified whereas the genomes of *A. baylyi* and *A. baumannii* harbored 14 and 19 predicted transposase-related genes, respectively. In *A. calcoaceticus*, transposase was not predicted by gene annotation. A low abundance of IS elements and transposases may be the reason for the relatively large size of the DR1 genome, as genome size reduction may be attributable to recombination and gene disruption mediated by IS elements and transposition events. The occurrence of natural transformation in strain DR1 has been previously confirmed (30). The genes required for natural competence, *comABCEF*, *comMNOLQ*, and *pilBCD*, are clustered in DR1, *A. baylyi*, *A. calcoaceticus* and *A. baumannii*, thereby suggesting that natural competence is a conserved trait of *Acinetobacter* species (3; see also Table S2 in the supplemental material). Putative horizontally transferred genes and clustered, regularly interspaced, short palindromic repeats (CRISPRs) have been determined and are included in the IMG database. (Relevant information concerning *A. calcoaceticus* PHEA-2, including that involving horizontally transferred genes and CRISPRs, was not available in the IMG database). Strain DR1, *A. baumannii*, and *A. baylyi* were estimated to harbor 114, 47, and 275 horizontally transferred genes, respectively. *Enterobacteriales* species are commonly the most prominent source of horizontally transferred genes in the three strains. CRISPRs were found only in the *A.*

baylyi genome. Three CRISPRs were closely located along the chromosome (bp 2339398 to 2339727, with 7 repetitions of 28 bp; bp 2371799 to 2373027, with 22 repetitions of 28 bp; and bp 2448115 to 2453544, with 91 repetitions of 28 bp). However, *cas*, a gene that is frequently associated with CRISPRs, was not detected in *A. baylyi*. In order to search for evidence of horizontal gene transfer, the GC content of the genome of strain DR1 was assessed using GC-Profile software (11; see also Fig. S3 in the supplemental material). The GC content of the genomic region, located at bp 808876 to 820186 (11.3 kb), was 50.1% (versus the overall average of 38.7%); surprisingly, no ORF was identified therein. Speculation regarding the origin of this intergenic region was impaired by the failure to obtain BLAST matches and to identify transposition-related sequences within the flanking regions.

Biofilm- and capsule-related sequences and homologues were searched on the basis of the results reported by Vallenet et al. (35). Sequences of type IV pili, flagella, curli, fimbriae, and chaperone usher secretion systems are classified into this group (see Table S3 in the supplemental material). Only half of the DR1 sequences retrieved are conserved in the three other strains. However, this is attributable to low levels of similarity or coverage between sequences, as opposed to the absence of relevant genes. Antibiotics and metal resistance genes were classified using the RAST server (see Table S4 in the supplemental material). Almost all genes were found to be shared by the four strains, suggesting that the resistance mechanism is more commonly shared in *Acinetobacter* species than other functions, such as those of phage-related proteins, biofilm and capsule functions, and natural transformation. The relationship between the presence of resistance genes and the extent of actual resistance remains unexploited thus far in this analysis.

Two copies of alkane 1-monooxygenase (encoded by *alkB* [AOLE_10550 and AOLE_13390]) are present in the DR1 genome. The amino acid sequence similarity of the two proteins was 63%. The protein encoded by AOLE_10550 evidences high amino acid sequence similarity to *A. baylyi* alkane monooxygenase (83.0%), whereas that encoded by AOLE_13390 evidences 59.9% similarity. The alkane monooxygenase of *Marinobacter aquaeolei* VT8 (Maqu_2843) is most closely related to the protein encoded by AOLE_13390 (CLSK927657) from another genus, according to the NCBI protein cluster database. Subsequent alkane metabolisms are likely mediated by alcohol dehydrogenase (encoded by AOLE_06670 and AOLE_09790) and aldehyde dehydrogenase (encoded by AOLE_06655). Expression of *alkB* during diesel utilization was previously confirmed (20).

The β-ketoadipate pathway is responsible for the degradation of various aromatic compounds. *catMBCAIJFD* genes are known to be responsible for the catechol branch of the β-ketoadipate pathway in strain DR1. Similar gene organizations have been detected in *A. baylyi*, *A. calcoaceticus*, and *A. baumannii*. The only difference is that *catA* (coding for catechol 1,2-dioxygenase) is located upstream of *catM*, encoding the LysR-type transcriptional regulator, with the two separated by two hypothetical genes (see Fig. S4A in the supplemental material). The protocatechuate branch of the β-ketoadipate pathway is encoded by *pcaIJFBDKCHG* in DR1. However, *pcaU*, the gene encoding the IclR-type transcriptional regulator, is not adjacent to the *pca* cluster in DR1, *A. calcoaceticus*, and *A.*

baumannii, in contrast to *A. baylyi*. The best BLAST matches to *A. baylyi pcaU* were AOLE_08475, BDGL_001353, and A1S_1875, which are separated from the *pca* clusters in DR1, *A. calcoaceticus*, and *A. baumannii*, respectively (see Fig. S4B in the supplemental material). Scattered *pca* genes have also been detected in *Pseudomonas putida* KT2440, *Polaromonas* sp. JS666, and *Pseudomonas stutzeri* A1501 and are expected to correspond to regulatory mechanisms different from those of *A. baylyi* (14, 25, 26).

Various pathways for the degradation of aromatic compounds are suggested by the genome sequences of DR1. Benzoate is converted into catechol by benzoate 1,2-dioxygenase and proteins encoded by clustered genes (AOLE_13330 to AOLE_13360) (see Fig. S5 in the supplemental material). 4-Hydroxybenzoate is oxidized by 4-hydroxybenzoate-3-monooxygenase (encoded by AOLE_12025; *pobA*), resulting in protocatechuate (3,4-dihydroxybenzoate). The β-ketoadipate pathway is responsible for further metabolite catabolism. *pobR*, the gene encoding the 4-hydroxybenzoate hydroxylase transcriptional activator, is located upstream of *pobA* (see Fig. S5 in the supplemental material). The DR1 genome harbors all genes required for quinate metabolism in an arrangement similar to that seen with *A. baylyi*. Although quinate dehydrogenase is not predicted in the NCBI genome database, AOLE_08450 is highly expected to be a quinate dehydrogenase, according to results of BLAST searches performed with *quiA* of *A. baylyi* and of analyses of KEGG orthology, the MetaCyc pathway, the IMG ortholog cluster, and the NCBI protein cluster database (CLSK909370). The product of quinate metabolism is protocatechuate, which feeds into the β-ketoadipate pathway. Ferulate is a precursor of lignin; its metabolism in *Pseudomonas* sp. HR199 has been previously characterized (29). In *A. baylyi*, the *hca* operon is predicted to be responsible for ferulate catabolism. AOLE_13735 to AOLE_13780 are homologues of the *hca* genes and evidence high amino acid sequence similarity (approximately 76% to 86%; see Fig. S5 in the supplemental material). Vanillate is generated as a result of ferulate catabolism. Strain DR1 is likely to utilize ferulate via vanillin, in similarity to *P. putida* KT2440, which harbors *hcaB* in a similar gene arrangement (27). Genes responsible for vanillate metabolism in strain DR1 are clustered within a small region harboring intervening genes (AOLE_13695 to AOLE_13730; see Fig. S5 in the supplemental material). Initially, AOLE_13695 and AOLE_13700 were predicted to encode a hypothetical protein and a 4-hydroxybenzoate transporter, according to the NCBI genome database. However, a BLASTP search revealed that the proteins encoded by AOLE_13700 and AOLE_13695 show amino acid similarities of 74% and 86%, respectively, to the vanillate transporter encoded by *vanK* (ACIAD0982) and the putative porin for vanillate trafficking encoded by *vanP* (ACIAD0983). The oxidation of vanillate by the *vanA*-encoded protein generates protocatechuate, which is a substrate for the β-ketoadipate pathway.

The absence of naphthalene catabolic genes in the DR1 genome is consistent with its inability to grow on naphthalene as a substrate. Interestingly, gentisate 1,2-dioxygenase (encoded by *nagI*; AOLE_09100) is absent from the genomes of all sequenced *Acinetobacter* species, with the exception of strain DR1. Gentisate metabolism has been previously assessed in

Ralstonia sp. strain U2 and *Polaromonas naphthalenivorans* CJ2 as a component of naphthalene metabolism (13, 36, 39). In *Ralstonia* sp. strain U2, the genes responsible for gentisate metabolism are closely associated with other naphthalene catabolic genes (Fig. 3). In particular, the functions of *nagI*, *nagL*, and *nagK*, which encode gentisate 1,2-dioxygenase, maleylpyruvate isomerase, and acylpyruvate hydrolase, respectively, were experimentally confirmed. In *P. naphthalenivorans* CJ2, the *nag* genes are clustered in two chromosomal regions with two different transcriptional regulators. While a large cluster, *nagAaGHAbBFCQEDJI′*, harbors the genes involved in naphthalene metabolism, a small cluster, *nagIKL*, harbors a gene related to gentisate metabolism. The protein encoded by AOLE_09100 evidences high amino acid sequence similarities with that in strain CJ2 encoded by *nagI* (63%), that in strain CJ2 encoded by *nagI′* (63.6%), and that in strain U2 encoded by *nagI* (61.5%). An NCBI protein cluster search (using CLSK2395739, a cupin domain-containing protein) revealed that gentisate 1,2-dioxygenase proteins are conserved within the proteobacteria and that the closest match to this protein in strain DR1 was PsycPRwf_0738 in *Psychrobacter* sp. PRwf-1 (see Fig. S6 in the supplemental material). The LysR-type transcription regulator, *nagR*, in strain DR1 was upstream of *nagI* (Fig. 3B). For growth tests, *A. baylyi* B2^T (= KACC 12224^T = DSM 14961^T = CCUG 50765^T), *A. baylyi* ADP1 (= ATCC 33305), *A. baumannii* ATCC 19606^T (= KCTC 2508^T = CCUG 19096^T = DSM 30007^T), and *A. baumannii* 17978 (= LMG 1025) were purchased from the Korean Agricultural Culture Collection (KACC), American Type Culture Collection (ATCC), Korean Collection for Type Culture (KCTC), and Belgian Co-ordinated Collections of Microorganisms (BCCM), respectively. Five bacterial strains were cultured in minimal salt basal (MSB) medium (34) supplemented with 2 mM gentisate at 30°C, with shaking at 220 rpm. As a result of the growth test, we confirmed two of strain DR1's distinctive physiological attributes: beginning at the same initial cell density as the other four cultures, strain DR1 grew to a high optical density (OD) within 10 h on both gentisate and salicylate and *A. baumannii* ATCC 17078 and ATCC 19606^T did not grow on either carbon source whereas *A. baylyi* ADP1 and B2^T exhibited increases in OD values in growth on salicylate (see Fig. S7 in the supplemental material). The protein encoded by AOLE_09105 (*nagX*; Fig. 3B) evidenced an amino acid sequence similarity of 76% to the 3-hydroxybenzoate 6-hydroxylase of strain CJ2, whereas no significant match was detected in other *Acinetobacter* species or strain U2. Strangely, the genes downstream of the gentisate cluster in strain DR1 (AOLE_09110 and AOLE_09115) have been predicted to encode maleylacetoacetate isomerase and fumarylacetoacetate hydrolase, which function in homogentisate metabolism. Further experiments were conducted to characterize *nagI* and the downstream genes of strain DR1, since AOLE_00310 to AOLE_00320 have been shown to be responsible for homogentisate metabolism in another part of the strain DR1 chromosomal structure.

Based on the ability to utilize gentisate and similar aromatic compounds, such as 3,4-dihydroxybenzoate, 3-hydroxybenzoate, 4-hydroxybenzoate, benzoate, and salicylate, expression of *nagR*, *nagI*, and *salA* (encoding salicylate 1-monooxygenase; AOLE_06150) in strain DR1 grown on gentisate was quanti-
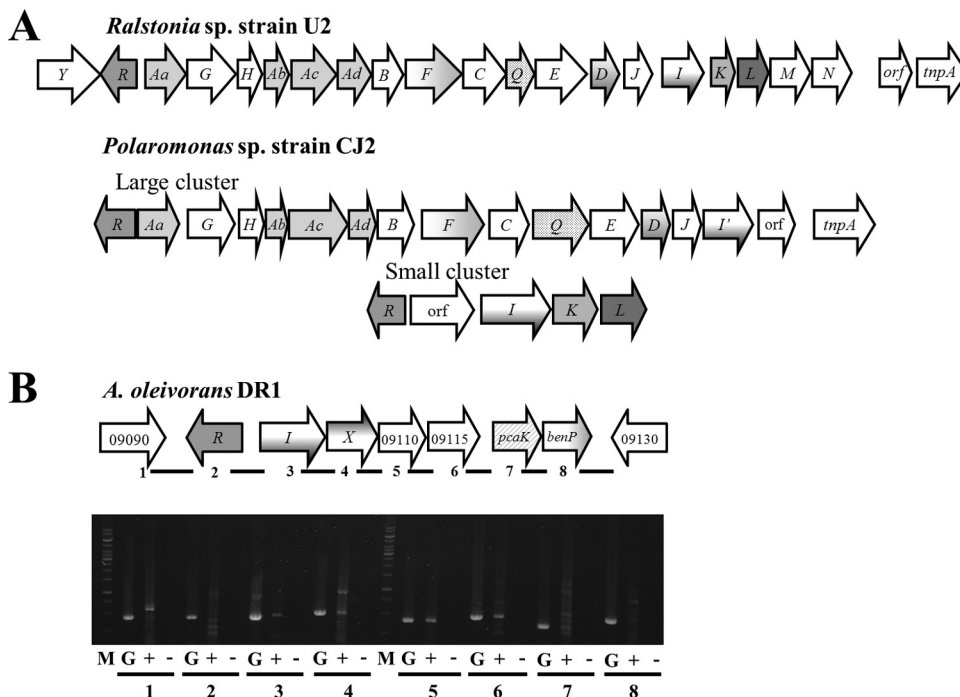
FIG. 3. Gentisate 1,2-dioxygenase (*nagI*) gene occurrence in archetypal strains (*Ralstonia* and *Polaromonas*) and in strain DR1. (A) The *nag* operons responsible for naphthalene metabolism in *Ralstonia* sp. strain U2 and *Polaromonas* sp. strain CJ2 are shown. (B) Cotranscription of the *nag* operon in strain DR1. Lines under arrows indicate the amplified intergenic-region PCR products from genomic DNA (G), cDNA (+), and the negative controls (− [no reverse transcriptase added]). M, 1-kb DNA ladder.

tatively assessed (Fig. 4). RNA was isolated from a culture exponentially grown to an OD at 600 nm (OD_{600}) of 0.3 in MSB medium containing 2 mM each carbon source. The PCR mixture contained 12.5 μl of iQ SYBR green Supermix (Bio-Rad), 1 μl of each primer (0.5 μM), and 1.5 μl of cDNA, in a total volume of 25 μl. The PCR conditions were 95°C for 3 min followed by 40 cycles of 45 s at 95°C, 45 s at 60°C, and 45 s at 72°C. The apparent upregulation of *nagR* and *nagI* in gentisate-utilizing cells was noted, thereby implying that *nagR* is involved in the regulation of gentisate metabolism and that *nagI* actually functions in gentisate catabolism. The significant upregulation of *nagR* in gentisate-utilizing cells indicates that

nagR in strain DR1 exerts a positive control effect during gentisate metabolism, as is also the case in *Polaromonas naphthalenivorans* CJ2 (13).

Although the functions of genes downstream of *nagI* are predicted to be related to homogentisate metabolism, the results of our growth tests and gene expression analyses raised some doubts as to the accuracy of our annotations. Therefore, we attempted to obtain detailed information to relate the functionality of genes downstream of *nagI* to gentisate metabolism by examining cotranscription. cDNA was synthesized with RNA isolated from gentisate-utilizing DR1 cells, according to the upregulation of *nagI*. Primers were designed to amplify the intergenic regions of the *nagI* and adjacent genes (see Table S5 in the supplemental material). Amplified PCR products of the intergenic regions determined cotranscription from *nagI* (AOLE_09100) to 4-hydroxybenzoate transporter-encoding *pcaK* (AOLE_09120) (Fig. 3B). This result is similar to that previously observed in analysis of strain CJ2, showing cotranscription corresponding to the small cluster harboring one upstream ORF, *nagI'KL*, and three downstream ORFs (14). In order to confirm the actual functions of AOLE_09110 and AOLE_09115, biochemical evidence would be required. However, we cautiously suggest that the *nagI* and 4 downstream genes function in gentisate metabolism and the results of related growth tests and gene expression and cotranscription analyses may indicate false predictions.

In conclusion, a comparison of four *Acinetobacter* genomes identified key commonalities and contrasts, including strain-specific genomic regions with unique characteristics, such as
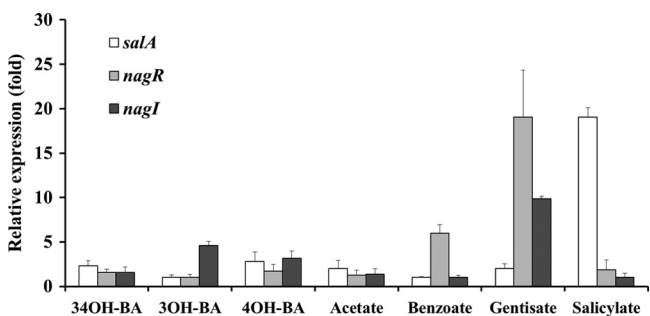

FIG. 4. Expression of *salA*, *nagR*, and *nagI* genes during growth of strain DR1 on 2 mM 3,4-dihydroxybenzoate (34OH-BA), 3-hydroxybenzoate (3OH-BA), 4-hydroxybenzoate (4OH-BA), acetate, benzoate, gentisate, or salicylate. The results were obtained from three independent experiments and normalized to 16S rRNA gene expression.

transport systems and bacteriophage-like sequences, in strain DR1. We hypothesize that strain DR1's large genome size may be attributable to gene incorporation events (based on the phage-like sequence and natural competence-related genes) in combination with a relatively low rate of gene loss, as predicted from the observed low abundances of IS elements and transposition-associated sequences in the genome of strain DR1. Even though the DR1 genome evidenced similarities to the *A. baylyi* genome that were relatively lower than those seen with *A. calcoaceticus* and *A. baumannii*, important gene clusters related to the degradation of aromatic compounds were conserved across all four genomes. Therefore, the ability to utilize diverse aromatic compounds may be an important common trait of *Acinetobacter* species. Although gentisate metabolism has not previously been associated with *Acinetobacter* species, herein we provided both bioinformatic and experimental evidence for gentisate utilization in strain DR1. Genomic and physiological analyses of strain DR1 and its relatives are aimed at providing essential information to promote further understanding of *Acinetobacter* species, particularly their environmental functions and impact.

REFERENCES

1. **Adams, M. D., et al.** 2008. Comparative genome sequence analysis of multidrug-resistant *Acinetobacter baumannii*. J. Bacteriol. **190:**8053–8064.
2. **Arber, W.** 2000. Genetic variation: molecular mechanisms and impact on microbial evolution. FEMS Microbiol. Rev. **24:**1–7.
3. **Averhoff, B., and A. Friedrich.** 2003. Type IV pili-related natural transformation systems: DNA transport in meshphilic and thermophilic bacteria. Arch. Microbiol. **180:**385–393.
4. **Barbe, V., et al.** 2004. Unique features revealed by the genome sequence of *Acinetobacter* sp. ADP1, a versatile and naturally transformation competent bacterium. Nucleic Acids Res. **32:**5766–5779.
5. **Braun, V., and K. Hantke.** 2011. Recent insights into iron import by bacteria. Curr. Opin. Chem. Biol. **15:**328–334.
6. **Dams-Kozlowska, H., M. P. Mercaldi, B. J. Panilaitis, D. L. Kaplan.** 2008. Modifications and applications of the *Acinetobacter veneianus* RAG-1 exopolysaccharide, the emulsan complex and its components. Appl. Microbiol. Biotechnol. **81:**201–210.
7. **Darling, A. C. E., B. Mau, F. R. Blattner, and N. T. Perna.** 2004. Mauve: multiple alignment of conserved genomic sequence with rearrangements. Genome Res. **14:**1394–1403.
8. **Dietrich, L. E., A. Price-Whelan, A. Petersen, M. Whiteley, and D. K. Newman.** 2006. The phenazine pyocyanin is a terminal signaling factor in the quorum sensing network of *Pseudomonas aeruginosa*. Mol. Microbiol. **61:**1308–1321.
9. **Dietrich, L. E., T. K. Teal, A. Price-Whelan, and D. K. Newman.** 2008. Redox-active antibiotics control gene expression and community behavior in divergent bacteria. Science **321:**1203–1206.
10. **Fournier, P. E., et al.** 2006. Comparative genomics of multidrug resistance in *Acinetobacter baumannii*. PLoS Genet. **2:**e7.
11. **Gao, F., and C. T. Zhang.** 2006. GC-Profile: a web-based tool for visualizing and analyzing the variation of GC content in genomic sequences. Nucleic Acids Res. **34:**W686–W691.
12. **Geissdörfer, W., R. G. Kok, A. Ratajczak, K. J. Hellingwerf, and W. Hillen.** 1999. The genes *rubA* and *rubB* for alkane degradation in *Acinetobacter* sp. strain ADP1 are in an operon with *estB*, encoding an esterase, and *oxyR*. J. Bacteriol. **181:**4292–4298.
13. **Jeon, C. O., M. Park, H. Ro, W. Park, and E. L. Madsen.** 2006. The naphthalene catabolic (*nag*) genes of *Polaromonas naphthalenivorans* CJ2:

14. evolutionary implications for two gene clusters and novel regulatory control. Appl. Environ. Microbiol. **72:**1086–1095.
14. **Jiménez, J. I., B. Minambres, J. L. Garcia, and E. Diaz.** 2002. Genomic analysis of the aromatic catabolic pathways from *Pseudomonas putida* KT2440. Environ. Microbiol. **4:**824–841.
15. **Jung, J., J. Baek, and W. Park.** 2010. Complete genome sequence of the diesel-degrading *Acinetobacter* sp. strain DR1. J. Bacteriol. **192:**4794–4795.
16. **Jung, J., J. Noh, and W. Park.** 2011. Physiological and metabolic responses for hexadecane degradation in *Acinetobacter oleivorans* DR1. J. Microbiol. **49:**208–215.
17. **Juni, E.** 1978. Genetics and physiology of *Acinetobacter*. Annu. Rev. Microbiol. **32:**349–371.
18. **Kang, Y. S., J. Jung, C. O. Jeon, and W. Park.** 2011. *Acinetobacter oleivorans* sp. nov. is capable of adhering to and growing on diesel-oil. J. Microbiol. **49:**29–34.
19. **Kang, Y. S., and W. Park.** 2010a. Contribution of quorum-sensing system to hexadecane degradation and biofilm formation in *Acinetobacter* sp. strain DR1. J. Appl. Microbiol. **109:**1650–1659.
20. **Kang, Y. S., and W. Park.** 2010b. Protection against diesel oil toxicity by sodium chloride-induced exopolysaccharides in *Acinetobacter* sp. strain DR1. J. Biosci. Bioeng. **109:**118–123.
21. **Kang, Y. S., and W. Park.** 2010c. Trade-off between antibiotic resistance and biological fitness in *Acinetobacter* sp. strain DR1. Environ. Microbiol. **12:**1304–1318.
22. **Kok, R. G., et al.** 1995. Characterization of the extracellular lipase, LipA, of *Acinetobacter calcoaceticus* BD413 and sequence analysis of cloned structural gene. Mol. Microbiol. **15:**803–818.
23. **Kwan, T., J. Liu, M. DuBow, P. Gros, and J. Pelletier.** 2005. The complete genomes and proteomes of 27 *Staphylococcus aureus* bacteriophages. Proc. Natl. Acad. Sci. U. S. A. **102:**5174–5179.
24. **Kwan, T., J. Liu, M. DuBow, P. Gros, and J. Pelletier.** 2006. Comparative genomic analysis of 18 *Pseudomonas aeruginosa* bacteriophages. J. Bacteriol. **188:**1184–1187.
25. **Li, D., et al.** 2010. Genome-wide investigation and functional characterization of the β-ketoadipate pathway in the nitrogen-fixing and root-associated bacterium *Pseudomonas stutzeri* A1501. BMC Microbiol. **10:**36.
26. **Mattes, T. E., et al.** 2008. The genome of *Polaromonas* sp. strain JS666: insight into the evolution of a hydrocarbon- and xenobiotic-degrading bacterium, and features of relevance to biotechnology. Appl. Environ. Microbiol. **74:**6405–6416.
27. **Nelson, K. E., et al.** 2002. Complete genome sequence and comparative analysis of the metabolically versatile *Pseudomonas putida* KT2440. Environ. Microbiol. **4:**799–808.
28. **Novick, R. P., G. E. Christie, and J. R. Penadés.** 2010. The phage-related chromosomal islands of Gram-positive bacteria. Nat. Rev. Microbiol. **8:**541–551.
29. **Overhage, J., H. Priefert, and A. Steinbüchel.** 1999. Biochemical and genetic analysis of ferulic acid catabolism in *Pseudomonas* sp. strain HR199. Appl. Environ. Microbiol. **65:**4837–4847.
30. **Park, J., and W. Park.** 2011. Phenotypic and physiological changes in *Acinetobacter* sp. strain DR1 with exogenous plasmid. Curr. Microbiol. **62:**249–254.
31. Reference deleted.
32. **Pedulla, M. L., et al.** 2003. Origins of highly mosaic mycobacteriophage genomes. Cell **113:**171–182.
33. Reference deleted.
34. **Stanier, L. Y., N. J. Palleroni, and M. Douderoff.** 1966. The aerobic pseudomonads: a taxonomic study. J. Gen. Microbiol. **43:**159–271.
35. **Vallenet, D., et al.** 2008. Comparative analysis of *Acinetobacters*: three genomes for three lifestyles. PLoS One **3:**e1805.
36. **Yagi, J. M., D. Sims, T. Brettin, D. Bruce, and E. L. Madsen.** 2009. The genome of *Polaromonas naphthalenivorans* strain CJ2, isolated from coal tar-contaminated sediment, reveals physiological and metabolic versatility and evolution through extensive horizontal gene transfer. Environ. Microbiol. **11:**2253–2270.
37. **Zarrilli, R., M. Crispino, and M. Bagattini.** 2004. Molecular epidemiology of sequential outbreaks of *Acinetobacter baumannii* in an intensive care unit shows the emergence of carbapenem resistance. J. Clin. Microbiol. **42:**946–953.
38. **Zhan, Y., et al.** 2011. Genome sequence of *Acinetobacter calcoaceticus* PHEA-2, isolated from industry wastewater. J. Bacteriol. **193:**2672–2673.
39. **Zhou, N., S. L. Fuenmayor, and P. A. Williams.** 2001. *nag* genes of *Ralstonia* (formerly *Pseudomonas*) sp. strain U2 encoding enzymes for gentisate catabolism. J. Bacteriol. **183:**700–708.